INTERNATIONAL JOURNAL OF
COASTAL, OFFSHORE & ENVIRONMENTAL ENGINEERING IJCOE Vol.7/No. 2/Spring 2022 (1-10)

Available online at: www. Ijcoe.org

Inter-comparison of single-sensor and merged multi-sensor ocean color chlorophyll-a products in the shallow turbid waters - case study: Persian Gulf

Masoud, Moradi

Iranian National Institute of Oceanography and Atmospheric Science, moradi_msd@yahoo.com

ARTICLE INFO

Article History:
Received: 15 Dec. 2021
Accepted: 15 Mar. 2022

Keywords:
Remote sensing
Phytoplankton
Spatial coverage
Complex waters
Dusty atmosphere

ABSTRACT

Ocean color satellite sensors provide the only long-term Essential Climate Variable (ECV) globally that targets Chlorophyll-a concentrations (Chl-a) as the most important biological factor in the oceans. It is difficult to develop the long-term and consistent ocean color time-series for climate studies due to the differences in characteristics, atmospheric correction, Chl-a retrieval algorithms, and limited lifespans of individual satellite sensors. Therefore, the merged multi-sensor ocean color datasets were developed by merging data from different satellite sensor products. The performance of the commonly used single-sensor and multi-sensor merged ocean color datasets is a challenging issue over highly turbid coastal waters and dusty atmospheric conditions. In this study, we compared the common single-sensor [Sea-viewing Wide Field-of-view Sensor (SeaWiFS), Moderate Resolution Imaging Spectroradiometer (MODIS), Medium Resolution Imaging Spectrometer (MERIS), Visible Imager Radiometer (VIIRS), and Sentinel-3 Ocean and Land Colour Instrument (OLCI)], and merged multi-sensor [Ocean Colour Climate Change Initiative (OC-CCI), and GlobColour weighted average (GC-AVW) and Garver-Siegel-Maritorena (GC-GSM)] Chl-a datasets over the Persian Gulf, known as optically complex and highly turbid water bodies in a dusty atmospheric condition. The results indicate that the OC-CCI dataset provides more spatial and temporal coverages than the other datasets. Temporal consistency between single-sensor and merged datasets was made in two different timespans during the common period of sensors and during the continuous lifespan intersection between individual two-paired of datasets. The statistical metrics were calculated to show the temporal consistency between Chl-a datasets during the common and continuous time periods. Correlation between OC-CCI and the other datasets showed that the relationships between datasets did not change significantly during the proposed time periods. Further, it was indicated that the OC-CCI product is more constant than the other single-sensor and merged products. It was shown that OC-CCI datasets were more consistent with MERIS and GC-GSM datasets, and SeaWiFS and GC-AVW were not significantly correlated to the other datasets. The results revealed that the single sensor products that use POLYMER atmospheric correction algorithm (e.g. MERIS), and merged multi-sensor product that performs the GSM blending algorithms (e.g. GC-GSM) are more consistent and stable than the other products over the study area.

1. Introduction

Marine phytoplankton display a great role in the cycling of other elements in the marine environments including iron, silica, nitrogen, nitrate, and phosphate [1]. They also consume carbon dioxide and control the cycling of carbon over global oceans [2]. Knowledge of phytoplankton variations and abundances is used to predict the impact of marine ecosystem on climate variability and climate change [3]. Hence, monitoring of phytoplankton variations with proper temporal and spatial resolutions is an imperative task for climate change and marine ecosystem studies [4].

Ocean color has been indicated as an Essential Climate Variable (ECV) for climate research purposes [4]. In this regard, ocean color datasets should be sustainable at least over a few decades because of decadal

variability of oceanic factors [5,6]. Ocean color remote sensing is the only available technique for monitoring of phytoplankton on synoptic scales, and it provides time-series datasets of chlorophyll-a concentration (Chl-a) as an indicator of phytoplankton abundances. However, ocean color satellite sensors have limited lifespans typically about 10 years, and visible spectral radiometry, which is used for ocean color estimations, needs to be improved. This type of improvements includes: failure to identify the source of errors related to the main features retrieved by standard methods, reduction of consistency in data due to the different spectral characteristics of sensors performed in successive mission, occurrence of missing data, gaps in datasets, limited duration of each satellite mission. Therefore, continuous time-series ocean color data are required to be merged from different satellite missions as seamless data and free of artificial gaps, missing data, and trends which rise from blending of disparate ocean color datasets.

European Space Agency (ESA) developed the first ocean color blended time series from different single satellite sensors in 2010, known as Ocean Colour Climate Change Initiative (OC-CCI). The OC-CCI has generated globally by merging observations from Sea-viewing Wide Field-of-view Sensor (SeaWiFS), Moderate Resolution Imaging Spectroradiometer (MODIS), and Medium Resolution Imaging Spectrometer (MERIS) satellite sensors [4]. The final version of OC-CCI has been corrected for inter-sensor biases and all radiometric bands shifted to the bands of SeaWiFS. The OC-CCI performs the POLYMER atmospheric correction algorithm applied to MERIS and MODIS [7]. Similarly, the Copernicus Marine Environment Service (CMEMS) has developed a regular dataset for marine ecosystems globally on the physical state of marine environment including temperature, currents, salinity, sea surface height, sea ice, marine optical properties, and ocean color chlorophyll-a concentrations (known as GlobColour) [8]. The GlobColour merged Chl-a products have been generated based on observations from SeaWiFS, MERIS, MODIS, Visible Imager Radiometer (VIIRS), and Sentinel-3 Ocean and Land Colour Instrument (OLCI). GlobColour has performed different algorithms to retrieve Chl-a from reflectance data. It uses three algorithms including: the Ocean Color Index (OCI) algorithm for oligotrophic waters (9), common NASA OCX (OC3 and OC4) algorithms depending on the sensor, and the OC5 algorithm [10] for coastal complex waters. The OC-CCI and GlobColour datasets are available from 1997 to present and provide fewer missing data than any other single sensor ocean color dataset. They both use OC5 and OCI Chl-a retrieval algorithms over complex turbid waters [8], and often provide relatively similar datasets in the coastal waters, although some differences exist because of the merging and flagging approaches. The OC5 and OCI retrieval algorithms have been developed for SeaWiFS, MERIS, MODIS, VIIRS, and OLCI sensors over the complex water bodies. Therefore, merged multi-sensor and single-sensor Chl-a products are available in the complex turbid coastal water bodies with similar retrieval algorithms.

Comparing the OC-CCI and GlobColour datasets with those available from single sensor data in the coastal complex waters provide required information for adopting the most reliable Chl-a data for studying the phytoplankton dynamics from all available ocean color datasets. However, the accuracy of long-term merged and single sensors Chl-a datasets in the complex water bodies remains as a challenging issue. Furthermore, comparison of merged multi-sensor with single-sensor Chl-a datasets contributes to give some insight on the uncertainties affecting the Chl-a products in the coastal turbid waters. In this article, we evaluate the performance of OC-CCI and GlobColour merged multi-sensor Chl-a datasets with other existing single-sensor (SeaWiFS, MERIS, MODIS, VIIRS, and OLCI) satellite-derived Chl-a using OCI and OC5 algorithms in the highly turbid complex waters of the Persian Gulf. We focus on the instabilities in the merged Chl-a products that rise from merging and flagging of merged multi-sensor observations, and demonstrate the consistency between different Chl-a datasets which have been estimated using similar retrieval algorithms (OC5 and OCI).

2. Data and Methods

2.1. Satellite data

The Chl-a datasets used in this study comprise from monthly different single-sensor and merged multi-sensor satellite datasets with spatial resolution 4km during 1997-2020. The single-sensor datasets were obtained from National Aeronautics and Space Administration (NASA) ocean color website (http://oceandata.sci.gsfc.nasa.gov/) during their mission lifespans including: SeaWiFS (1997-2010), MERIS (2002-2012), MODIS (2002-2020), VIIRS (2012-2020), and OLCI (2016-2020). The OC5 retrieval algorithm was performed to retrieve Chl-a from each of the selected satellite sensors during the time period.

Two different Chl-a datasets are available from GlobColour (hereafter known as GC) that differ in the merging techniques. The GlobColour provides the weighted average (GC-AVW) and the Garver-Siegel-Maritorena (GC-GSM) datasets. The daily Chl-a products from level-2 of the single-sensor datasets were computed and then the corresponding Chl-a from SeaWiFS and MODIS were adjusted to the Morel algorithm [11] to transforms the Chl-a data to the MERIS data [8]. The GC products performs the OC5 algorithms for Chl-a retrieval in the complex waters and utilizes Neural Network merging approaches to develop Level-3 gridded datasets [12]. The number of

valid pixels from each sensor was used as the weights in the merged products. The monthly datasets of both GC were downloaded from CMEMS website (http://www.globcolor.info) and transformed in local plate carree grid format with average spatial resolution of 4km.

The OC-CCI uses the OC5 and OCI retrieval algorithms to estimates Chl-a and performs the POLYMER atmospheric correction algorithm [4]. Hence, the Chl-a datasets of OC-CCI comprise high number of measurements from MERIS and show a better spatial coverage than the other single-sensor and/or merged products [8]. Here, the monthly of OC-CCI version 5.0 downloaded from ESA website (http://www.esa-ocean clour-cci.org) and then transformed in local plate carree grid format with average spatial resolution of 4km. The spatial and temporal resolution of merged multi-sensor and single sensor ocean color derived Chl-a datasets were matched for comparisons and further analysis.

2.2. Methods

The OC-CCI and GC datasets are compared with the corresponding records of single-sensor (SeaWiFS, MERIS, MODIS, VIIRS, and OLCI) Chl-a datasets pixel-by-pixel across the whole Persian Gulf. The bias (δ), unbiased root mean square (RMS) and its difference (Δu,RMS), mean ratio (φ), and correlation coefficient (r) are used to calculate the consistency between Chl-a datasets. These statistical indices are metrics commonly used for assessment and comparison evaluation of products of satellite-derived Chl-a [13]. The analyses were performed in two groups: (a) for common period with continuous observations that is no gaps in the monthly datasets in the purpose of assessing the similarity between each record, given: 2002-2010 for SeaWiFS, MERIS, MODIS, and merged-sensor datasets, and 2016-2020 for MODIS, VIIRS, OLCI, and merged-sensor datasets, and (b) for periods to any pair of datasets. The monthly Chl-a datasets were transformed to Log10 bases (here after will be shown as Log10(Chl-a)) before analyses to fully cover the log-normal distribution of these datasets [14]. The bias (δ) is calculated as bellow [15]:

$$\delta = \frac{1}{N}\sum_{i=1}^{n}[Log10(y_i) - Log10(x_i)] \quad (1)$$

where N is the total number of matched observations, y_i and x_i are the pairs of observations. The unbiased RMS ($\Delta_{u,RMS}$) is defined as [16]:

$$\Delta_{u.RMS} = \left(\frac{1}{N}\sum_{i=1}^{N}\{[log10(y_{2.i}) - \overline{log10(x_{2.i})}] - [log10(y_{1.i}) - \overline{log10(x_{1.i})}]\}\text{^}2\right)^{1/2} \quad (2)$$

The average values are shown with overbars. The mean ratio (φ) is defined as:

$$\emptyset = \frac{1}{N}\sum_{i=1}^{n}\frac{y_{2.i}}{y_{1.i}} \quad (3)$$

Unbiased RMS is defined as:

$$\text{RMS} = \sqrt{\frac{1}{n}\sum_{i=1}^{n}[Log10(y_i) - Log10(x_i)]^2} \quad (4)$$

The relationship between datasets are defined using the multiple statistical metrics defined above, that makes interpretation difficult. To do this, Target and Taylor diagrams are used to combine and summarize the results [16]. These diagrams have been widely used in remote sensing researches and represents one the most quantitate description of consistency between datasets [17–19]. Taylor diagram displays the standard deviation (σ), correlation coefficient (r), and unbiased RMS between pairs of data [20]. Target diagrams show the bias (δ) and Δu,RMS in a scatter polar plot [16].

The accurate consistency between two datasets are clearly indicated using time-series analysis of the unbiased differences between measurements of two different datasets [21]. Δu,RMS (equation 2) is used as a measure of consistency between two datasets, and the smaller values represent a more stable relationship.

3. Results

3.1. Spatial and temporal coverage

To compare the monthly Chl-a imageries from the selected single and merged-sensor, missing data were excluded from all satellite sensors. Only common grid pixels with valid measurements were used in the statistical analysis to minimize the influence of spatio-temporal bad sampling among datasets. However, we have to acknowledge that the effect of missed data would not have been entirely eliminated because there are desperate number of satellite sensor measurements due to differences in orbits and sampling rates which have been used by data providers to compute the monthly averages. Fig. 1 shows the percent of valid observation of each datasets over the entire period of each satellite mission, given that: SeaWiFS 1997-2010, MERIS 2002-2012, MODIS 2002-2020, VIIRS 2012-2020, OLCI 2016-2020, GC-GSM and GC-AVW 1997-2020, OC-CCI 1997-2020. The geographical distribution of valid measurements over grid point measurements seems to be regular, with the most valid

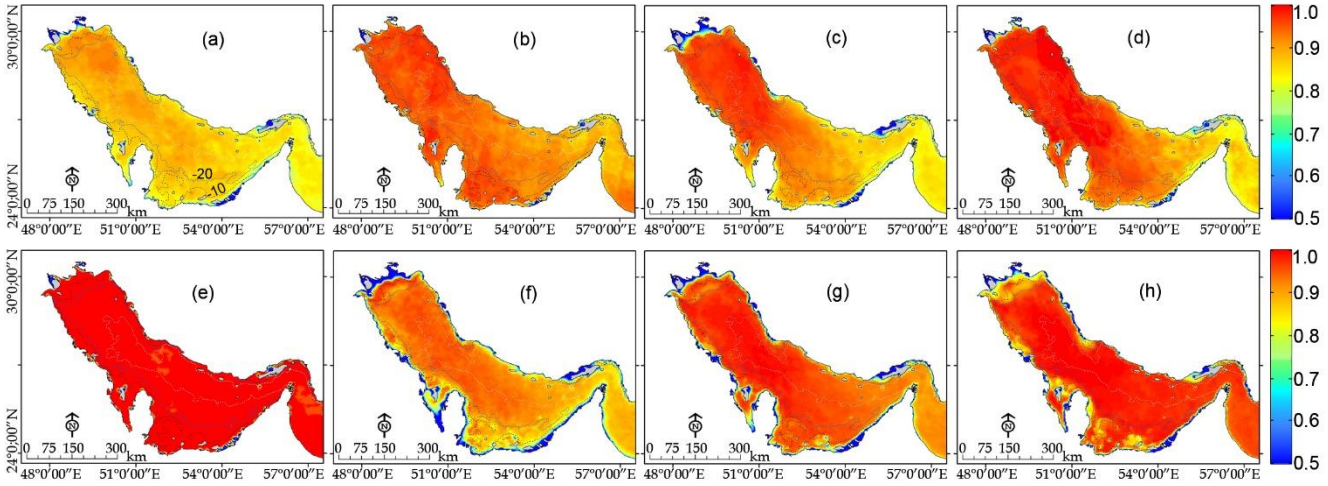

Figure 1. Spatial coverage of the percentage of valid measurements during the lifespan of each dataset. (a) SeaWiFS, (b) MERIS, (c) MODIS, (d) VIIRS, (e) OLCI, (f) GC-AVW, (g) GC-GSM, (h) OC-CCI. Overlaid dashed lines show isobaths. Color bars show percentage of the valid measurements, given bad observations and missing data eliminated.

points in the deeper areas and lowest valid points along coastal areas. Among the single sensor data sets, SeaWiFS (Fig. 1a) and OLCI (Fig. 1e) show the lowest and highest number of valid measurements in the deeper areas of the Persian Gulf, respectively. Among merged-sensor datasets, GC-GSM (Fig. 1g) and OC-CCI (Fig. 1h) show the highest (>0.93) and GC-AVW (Fig. f) shows the lowest (>0.84) percent of spatial coverage valid measurements. In all cases, the spatial coverage of valid data along the coastal regions (depth <10 m) are less than 0.65 of satellite measurements. Along the north-west regions of the Persian Gulf, the percentage of valid measurements is less than 0.55 for all of the datasets.

The number of valid monthly observations (N) of each Chl-a datasets across Persian Gulf during the study period are shown in Fig. 2. The N values of the single-sensor datasets are about 13600 for SeaWiFS, 13700 for MERIS, 13600 for MODIS, 13700 for VIIRS, and 13800 for OLCI. During the temporal coverage by merged datasets from 1997 to 2020, the number of valid monthly measurements increased greatly from mid-2002 onward. Before mid-2002, the N values of OC-CCI, GC-AVW, and GC-GSM were 12300, 12500, and 12200, respectively. After mid-2002, the N values of OC-CCI increased in average to 14200 till mid-2002, and then decreased to 13300. The N values of GC-AVW and GC-GSM reached in average to 13300 after mid-2002 and continued to the end of 2020. The OC-CCI uses the MERIS datasets as a reference of atmospheric correction (POLYMER) to blend the other sensor Chl-a data. Hence, during the lifespan of MERIS (Mid-2002 to 2012) the OC-CCI datasets show the greatest values of valid observations.

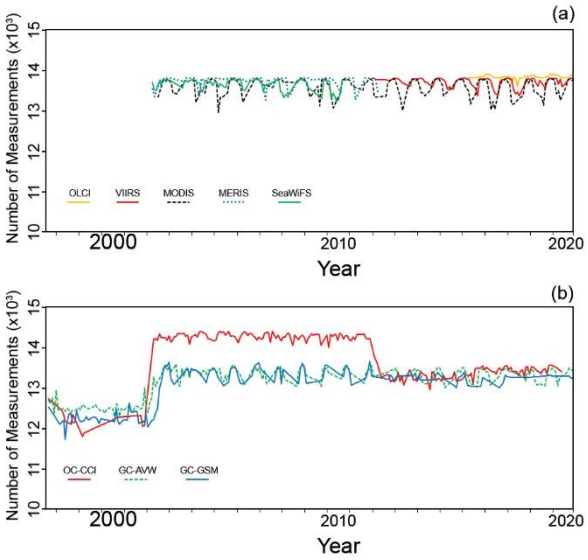

Figure 2. Temporal coverage of valid monthly measurement across grid pixels of Persian Gulf (Fig. 1) during the lifespan of single-sensor (a) and merged-sensor (b) datasets.

3.2. Comparison of Chl-a datasets in common periods

Here, we considered the common time periods as a frame of temporal coverage from July-2002 to Nov-2010 to compare SeaWiFS, MERIS, MODIS, and the three merged datasets, and from Apr-2016 to Dec-2020 to compare MODIS, VIIRS, OLCI, and the three merged datasets. Previous studies show that the OC-CCI datasets have the greatest correlation with in situ Chl-a measurements than the other single-sensor and merged datasets across the Persian Gulf [22]. Further, the OC-CCI shows the most temporal continuous valid monthly observations in the study area that covers the temporal coverages of the whole proposed common periods (Fig. 2). Therefore, we deem the OC-CCI as a baseline observation and calculate the statistical parameters according to this data.

Table 1. Statistical results of the spatially averaged between OC-CCI and selected single-sensor and all GC datasets during the common time periods. All correlations have been calculated for p<0.05, N is the number of matched common monthly observations between data pairs. P1% and P99% are the 1st and 99th percentiles.

Period	Dataset	φ	r	$\Delta_{u,RMS}$	δ	mean	σ	$P_{1\%}$	$P_{99\%}$	N
2002-2010	SeaWiFS	0.830	0.734	0.291	0.217	1.140	0.395	0.751	3.374	94
	MERIS	0.831	0.895	0.173	0.215	1.142	0.313	0.761	2.668	101
	MODIS	0.728	0.728	0.179	0.362	0.995	0.260	0.583	2.969	101
	GC-AVW	1.293	0.709	0.323	-0.411	1.769	0.248	1.086	3.833	101
	GC-GSM	0.618	0.872	0.174	0.505	0.852	0.466	0.426	3.668	101
2016-2020	MODIS	0.742	0.757	0.171	0.053	0.977	0.256	0.628	1.325	51
	VIIRS	0.784	0.789	0.114	0.219	0.811	0.185	0.578	1.425	51
	OLCI	1.085	0.695	0.116	-0.076	1.106	0.136	0.851	1.460	51
	GC-AVW	1.289	0.771	0.385	-0.318	1.348	0.498	0.810	1.103	51
	GC-GSM	0.619	0.878	0.083	0.384	0.645	0.175	0.356	1.089	51

The OC-CCI dataset showed the highest correlation with MERIS (r=0.89) among single-sensor datasets, and GC-GSM among the merged datasets (r=0.87) during the mid-2002 to mid-2010. The spatial average value of Chl-a during this time period was 1.358±0.176 mg m-3, the 1st percentile 0.587 mg m-3, and 99th percentile 3.946 mg m-3. The average and percentile values were closer to the corresponding value of merged datasets rather than those found in single-sensor statistical values. The significant Correlations (p<0.05) between OC-CCI and merged and single-sensor datasets were not robust enough (0.73>r>0.89), and differences were relatively big, given by Δu,RMS>0.1 and δ<0.1 (Table 1). In general, the similarity and lowest differences between OC-CCI were observed with MERIS among single-sensor, and GC-GSM among merged datasets.

During the second common period (Apr-2016 to end of 2020), the highest correlation was observed between OC-CCI and GC-GSM (r=0.88). The results of the comparison during the second common period is very similar to the firs common period, and differences between OC-CCI and single-sensor datasets are relatively high (Table 1). The spatial average value of Chl-a during this time period was 1.031±0.158 mg m-3, the 1st percentile 0.627 mg m-3, and 99th percentile 3.416 mg m-3. In general, the similarity and lowest differences between OC-CCI were observed with VIIRS among single-sensor, and GC-GSM among merged datasets during the time period 2016-2020.

Tylor diagram suggests an obvious similarity between OC-CCI and GC-GSM and MERIS than the other datasets (Fig. 3a, b). Comparison of OC-CCI with VIIRS and OLCI show an analogous result, and the GC-AVW showed to be the least similar dataset with OC-CCI. This analysis revealed that MODIS and SeaWiFS as the most dissimilar datasets to OC-CCI products among single-sensor records (Fig. 3a). The OC-CCI showed negative bias (δ) in relation to all datasets except OLCI and GC-AVW. The GC-AVW shows the greatest positive bias value to the OC-CCI. The both merged datasets, GC-AVW and GC-GSM, show the greater values of unbiased difference RMS (Δu,RMS) value to the OC-CCI in relation to the single-sensor datasets (Fig. 3c, d).

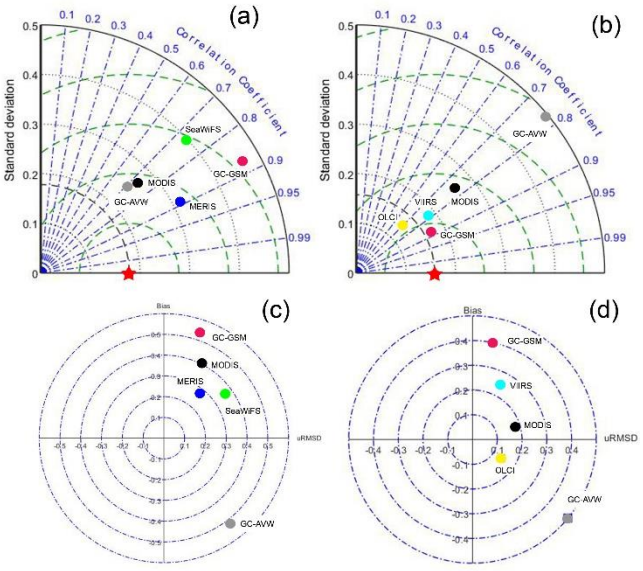

Figure 3. Taylor and Target diagram for common period observations from July-2002 to Nov-2010 (a, c), and from Apr-2016 to Dec-2020 (b, d) when comparing OC-CCI with single-sensor and merged monthly datasets.

Time-series of similarity metrics calculated using statistical correlation analysis between OC-CCI with the other datasets across the Persian Gulf at discrete time for each statistical metric. Time-series of all metrics showed strong interannual fluctuations during both proposed common periods (2002-2010 and 2016-2020). The timings of high and low peaks for each of the statistical metrics are not similar and depends on the target dataset (Fig. 4 and 5). Fig. 4 indicates that the

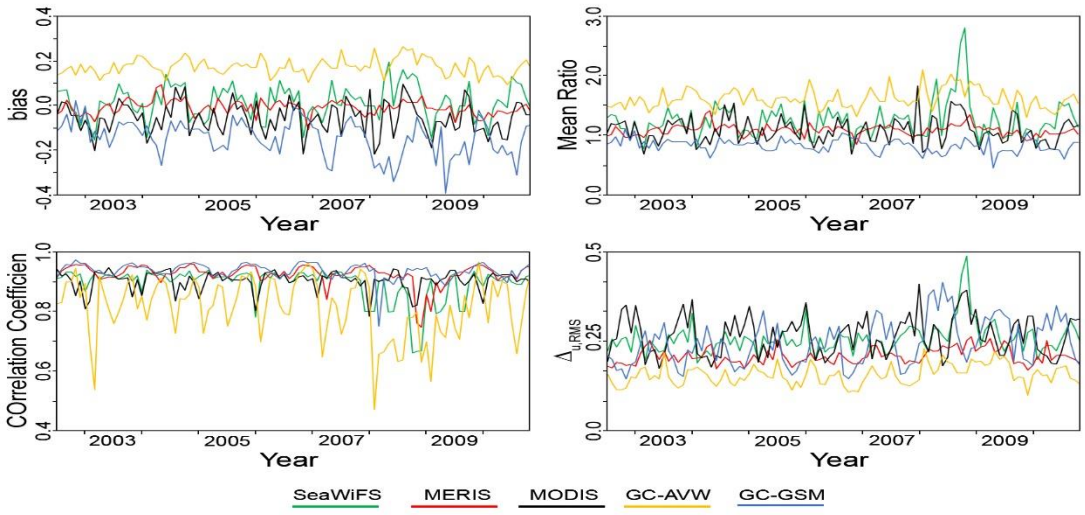

Figure 4. Time-series of statistical similarity metrics between OC-CCI, merged and single-sensor datasets during July-2002 to Nov-2010.

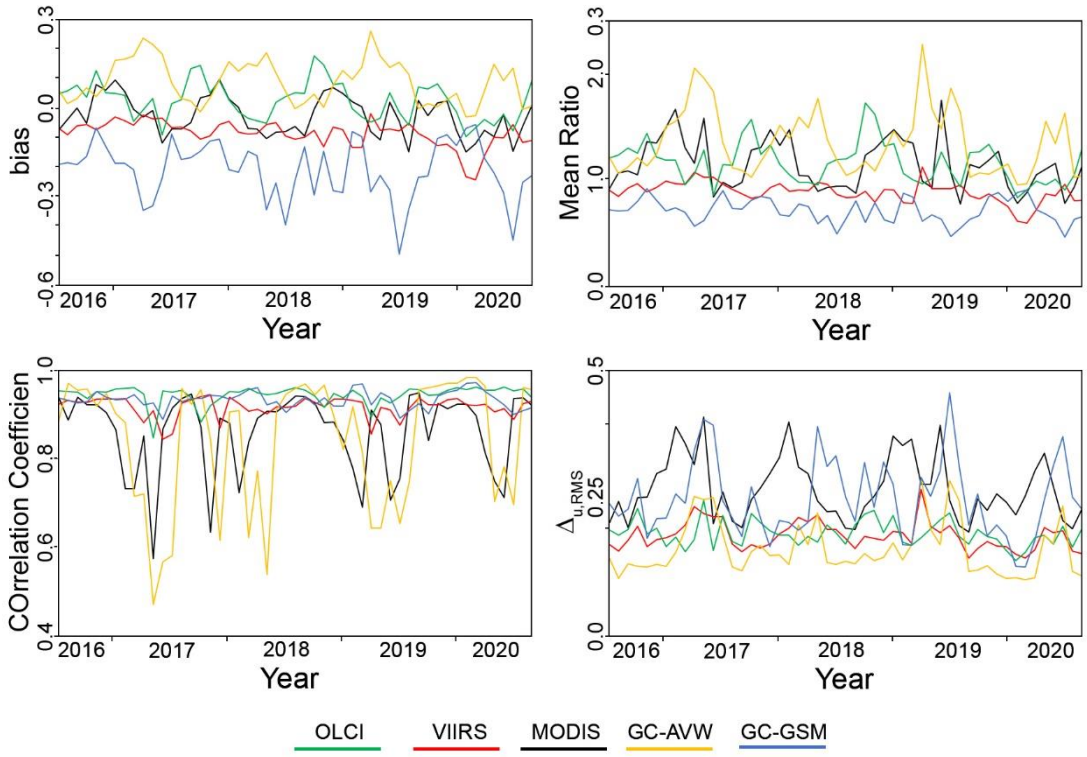

Figure 5. Time-series of statistical similarity metrics between OC-CCI, merged and single-sensor datasets during Apr-2016 to Dec-2020.

MERIS and GC-GSM datasets are the most similar datasets, and in contrast the GC-AVW and MODIS are the most different datasets when comparing with OC-CCI during 2002-2010. Similar results were obtained from time-series analysis of statistical metric during 2016-2020 (Fig. 5). During the summer, MODIS and GC-AVW showed higher values of Δu,RMS and bias (δ), and lower values of correlation coefficients relative to the other datasets during the both common periods (Fig. 4 and 5).

3.3. Comparison of Chl-a datasets in long-term period

Fig. 6 shows the spatially averaged time series of Chl-a values obtained from different single-sensor and merged datasets during the whole lifespan of all missions. All datasets show similar seasonal and interannual fluctuations, although the magnitude of peaks and troughs are not the same. A distinct peak is observed at late of 2008 which is correspond to the occurrence of a monstrous red tide in the Persian Gulf [23–25], and it has been detected in all merged and

single datasets. The results of statistical analysis of comparison between OC-CCI with the other datasets are shown in Table 2. The highest correlation was observed between OC-CCI and MERIS (r=0.87) among single-sensor datasets, and with GC-GSM (r=0.81) among merged datasets. The spatial average value of Chl-a from OC-CCI (1.119±0.176 mg m-3) and percentiles (0.587 mg m-3 for 1st, and 3.946 mg m-3 for 99th) (Table 2) are relatively equal to those found during the common periods (section 3.2). The worst correlation coefficient values and more differences between were observed between OC-CCI and MODIS (r=0.56, Δu,RMS=0.22) among single-sensor, and GC-AVW (r=0.33, Δu,RMS=0.30) among merged datasets (Table 2).

Temporal variability of Δu,RMS is a consistency metric of similarity between OC-CCI and the other merged and single-sensor datasets (section 2.2). Comparison between OC-CCI and the other datasets showed that temporal variations of Δu,RMS is strongly seasonal (Fig. 7), and it follows the interannual and trends of Chl-a time-series, which have been found previously over the Persian Gulf [26,27]. The GC-GSM among merged, and MERIS among single-sensor datasets showed the most stable and more consistent relationship with OC-CCI. There is a reasonable shift between Δu,RMS of GC-AVW and GC-GSM that suggests the similarity between merged datasets with OC-CCI are not stable among them and varies through time. The greatest shift of Δu,RMS between OC-CCI and merged datasets is observed concurrent to the lifespan of MERIS into the presented time-series. Before that both merged datasets use only SeaWiFS measurements, and therefore no notable shifts of Δu,RMS were observed. Introduction of more additional datasets into the merged datasets increase the number of observations (Fig. 2), and makes these datasets more robust. However, due to the different Chl-a blending algorithm of OC-AVW and GC-GSM, the stability of relationship with OC-CCI dataset are different and GC-GSM follows more robust and consistent trend with OC-CCI.

4. Discussion

In this study, we compared the merged multi-sensor and single-sensor datasets in the highly turbid and dusty environment of the Persian Gulf during 1997-2020. The OC-CCI dataset offers the most spatial/temporal coverage of Chl-a observations globally, given 22.9 billion in total and 127 million daily pixels. The accuracy of OC-CCI dataset across the world has been studied, and showed that it could be a best choice for ocean color data source among all of the available datasets [4,8,21]. In general, marginal seas and high turbid coastal waters show great inconsistency and uncertainties in both merged and single-sensor datasets. Furthermore, over the dusty shallow seas, such as Persian Gulf, the accuracy of ocean color data decreases significantly and it is necessary to evaluate the influence of atmospheric correction and Chl-a retrieval in these environments. We showed previously that the OC-CCI is more consistent then single-sensor datasets with in situ measurements, and also it is more similar than the other standard ocean color datasets with those produced by five band channels Chl-a retrieval algorithms customized for coastal complex waters [22]. Hence, the OC-CCI was selected as a baseline to evaluate the temporal consistency of the single-sensor and merged datasets across the dusty atmosphere and complex waters of the Persian Gulf. The finding of this study identifies indirectly the influence of atmospheric correction and retrieval algorithms on the accuracies of the available Chl-a data products. Thus, comparison between OC-CCI with the other available Chl-a datasets reveals the performance and applicability of ocean color datasets across the study area and similar marine environment.

The quality and robustness of Chl-a products may be depredated when data are merged. As an example, SeaWiFS, MERIS, and MODIS single-sensor datasets are consistent and robust over the open oceans, while OC-CCI products showed to be more similar to these products than OC-AVW dataset [18,21]. Therefore, merged ocean color datasets do not offer similar products, and their accuracies should be assessed. Here, we showed that OC-CCI datasets show more consistency with MERIS and GC-GSM datasets, and the week similarity was observed between SeaWiFS and GC-AVW datasets. While SeaWiFS is the reference sensor for OC-CCI data blending (see section 1), it does not show a notable similarity with OC-CCI across the Persian Gulf. In contrast, MERIS shows a significant and highest correlation and small value of unbiased difference, as well as the small bias value. Since SeaWiFS and OC-CCI perform the same Chl-a retrieval algorithm and similar wavebands to estimate Chl-a concentrations, the week similarity level shows the Chl-a retrieval algorithms are notable influenced by atmospheric and environmental factor. However, MERIS shows the highest level of similarity with OC-CCI, that indicate the performed atmospheric correction of MERIS datasets are highly significant over the dusty and hazy environment of Persian Gulf. Hence, the POLYMER atmospheric correction algorithm is significantly the most prominent criterion for this similarity among single-sensor datasets. The greatest differences were found between GC-AVW and OC-CCI (Fig. 3), and it could be likely due to the use of different algorithm for Chl-a estimation. Nevertheless, similarity between merged datasets (GC) are differ from each other more than expected, GC-AVW and GC-GSM show the worst and the best similarity, respectively. It is not surprising because the

Table 2. Statistical results of the spatially averaged between OC-CCI and selected single-sensor and all GC datasets during the common time period. All correlations have been calculated for p<0.05, N is the number of matched common monthly observations between data pairs. P1% and P99% are the 1st and 99th percentiles.

	SeaWiFS	MERIS	MODIS	VIIRS	OLCI	GC-AVW	GC-GSM	OC-CCI
φ	0.833	0.824	0.802	0.796	1.085	1.314	0.749	-
r	0.715	0.866	0.562	0.791	0.695	0.331	0.815	-
$\Delta_{u,RMS}$	0.219	0.162	0.221	0.099	0.116	0.297	0.294	-
δ	-0.087	-0.081	-0.105	-0.102	0.033	0.112	-0.049	-
mean	1.134	1.111	0.946	0.807	1.106	1.473	0.807	1.119
σ	0.393	0.290	0.242	0.161	0.136	0.469	0.248	0.261
$P_{1\%}$	0.752	0.725	0.557	0.581	0.851	0.773	0.381	0.587
$P_{99\%}$	3.350	2.554	1.785	1.304	1.460	3.029	3.511	3.946
N	97	121	216	102	51	274	274	-

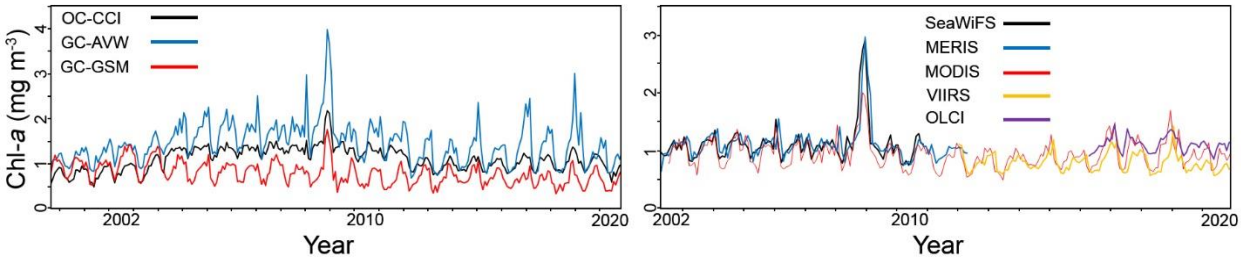

Figure 6. Time-series plot of spatially averaged of Chl-a across the Persian Gulf during the lifespan of merged (left) and single-sensor(right) datasets.

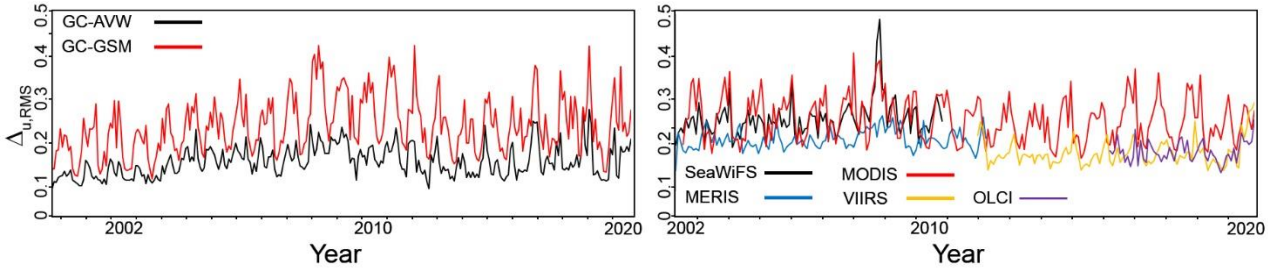

Figure 7. Time-series of Δu,RMS during the lifespan of merged and single-sensor datasets when comparing OC-CCI with merged (left) and single-sensor datasets (right).

two GC products are considerably different from each other in the atmospheric correction model, version of original data, and initial spatial resolution [4]. Therefore, it could be concluded that the proper atmospheric correction is more important than Chl-a retrieval algorithm in the dusty marginal seas such as Persian Gulf.

The merged datasets are produced using different blending algorithms to merge estimations of the different sources [8]. The presented results of this study suggests that the bias correction may increase the temporal consistency of the merged products, but our results do not recommend a distinct merging technique to enhance the long-term consistency. The comparison of two GC products yielded different results that could be due to the differences of both merging and flagging approaches [8,21]. However, all of the discrepancies between the single-sensor and merged products are expressed in the similarity between products and are reflected in the statistical metrics. Therefore, the results of this study present a rapid selection method for performing the available ocean color datasets, and it recommends the more accurate Chl-a datasets for the long-term studies across the Persian Gulf. Nevertheless, evaluating the performance of atmospheric correction and Chl-a retrieval algorithm across different climatic and environmental conditions in the dusty and complex marine environments remains a challenge.

5. Conclusions

This study addresses the inter-comparison of single-sensor and merged multi-sensor satellite-measured Chl-a over the optically complex and turbid waters under a dusty atmospheric condition of the Persian Gulf. The limited lifespan (10-year in average) of ocean color satellite sensors, beside the differences in their specifications, atmospheric correction and Chl-a retrieval algorithms make it difficult to create the long-term and consistent time-series ocean color datasets for climate change studies. Hence, creation of long-term datasets of near surface ocean color datasets is an essential task that achieved by merging the individual sensor missions to minimize the bias and uncertainties of single-sensor products. The OC-CCI dataset provides the most spatial and temporal coverages over the Persian Gulf during 1997 to 2020. Further, OC-CCI is the most prominent Chl-a record that matches the in situ measurements. Here, it was found that the OC-CCI dataset present a better performance in temporal robustness and consistency. The highest similarity and discrepancies between OC-CCI and the other Chl-a datasets were found with MERIS and GC-GSM, and SeaWiFS and GC-AVW, respectively. The results of this study showed that the single-sensor Chl-a datasets which performs the POLYMER atmospheric correction algorithm, and the merged multi-sensor products developed by GSM blending algorithm are the best choice of the Chl-a datasets over the Persian Gulf. However, further researches are recommended to assess the source and amount of uncertainties and discrepancies of atmospheric correction and Chl-a retrieval algorithms over the Persian Gulf.

Acknowledgment

This work has been supported by the Center for International Scientific Studies & Collaboration (CISSC), ministry of Science Research and Technology, Grant #990203. I express my gratitude to Dr. Masoud Sadreenasab, president of CISSC, for his kind cooperation.

6. References

[1] Platt T, Stuart V. (2008). *Why Ocean Colour? The Societal Benefits of Ocean-Colour Radiometry*. *vliz.be*. 1–8.

[2] Longhurst A, Sathyendranath S, Platt T, Caverhill C. (1995). *An estimate of global primary production in the ocean from satellite radiometer data*. Journal of Plankton Research. 17(6):1245–71.

[3] Muller-Karger FE, Kavanaugh MT, Montes E, Balch WM, Breitbart M, Chavez FP, et al. (2014). *A framework for a marine biodiversity observing network within changing continental shelf seascapes*. Vol. 27, Oceanography. p. 18–23.

[4] Sathyendranath S, Brewin RJ, Brockmann C, Brotas V, Calton B, Chuprin A, et al. (2019). *An ocean-colour time series for use in climate studies: The experience of the ocean-colour climate change initiative (OC-CCI)*. Sensors. 19(19):4285.

[5] Beaulieu C, Henson SA, Sarmiento JL, Dunne JP, Doney SC, Rykaczewski RR, et al. (2013). *Factors challenging our ability to detect long-term trends in ocean chlorophyll*. Biogeosciences. 10(4):2711–24.

[6] Racault MF, Le Quéré C, Buitenhuis E, Sathyendranath S, Platt T. (2012). *Phytoplankton phenology in the global ocean*. Ecological Indicators. 14(1):152–63.

[7] Steinmetz F, Deschamps P-Y, Ramon D. (2011). *Atmospheric correction in presence of sun glint: application to MERIS*. Optics Express. 19(10):9783.

[8] Garnesson P, Mangin A, D'Andon OF, Demaria J, Bretagnon M. (2019). *The CMEMS GlobColour chlorophyll a product based on satellite observation: Multi-sensor merging and flagging strategies*. Ocean Science. 15(3):819–30.

[9] Hu C, Lee Z, Franz B. (2012). *Chlorophyll a algorithms for oligotrophic oceans: A novel approach based on three-band reflectance difference.* Journal of Geophysical Research: Oceans. 117(1):1011.

[10] Gohin F, Druon JN, Lampert L. (2002). *A five channel chlorophyll concentration algorithm applied to Sea WiFS data processed by SeaDAS in coastal waters.* International Journal of Remote Sensing. 23(8):1639–61.

[11] Morel A, Huot Y, Gentili B, Werdell PJ, Hooker SB, Franz BA. (2007). *Examining the consistency of products derived from various ocean color sensors in open ocean (Case 1) waters in the perspective of a multi-sensor approach*. Remote Sensing of Environment. 111(1):69–88.

[12] Brewin RJW, Sathyendranath S, Müller D, Brockmann C, Deschamps PY, Devred E, et al. (2015). *The Ocean Colour Climate Change Initiative: III. A round-robin comparison on in-water bio-optical algorithms.* Remote Sensing of Environment. 162.

[13] Seegers BN, Stumpf RP, Schaeffer BA, Loftin KA, Werdell PJ. (2018). *Performance metrics for the assessment of satellite data products: an ocean color case study*. Optics Express. 26(6):7404.

[14] Campbell JW. (1995). *The lognormal distribution as a model for bio-optical variability in the sea*. Journal of Geophysical Research. 100(C7).

[15] Gregg WW, Casey NW, McClain CR. (2005). *Recent trends in global ocean chlorophyll*. Geophysical Research Letters. 32(3):1–5.

[16] Jolliff JK, Kindle JC, Shulman I, Penta B, Friedrichs MAM, Helber R, et al. (2009*). Summary diagrams for coupled hydrodynamic-ecosystem model skill assessment.* Journal of Marine Systems. 76(1–2):64–82.

[17] Saba VS, Friedrichs MAM, Antoine D, Armstrong RA, Asanuma I, Behrenfeld MJ, et al. (2011). *An evaluation of ocean color model estimates of marine primary productivity in coastal and pelagic regions across the globe*. Biogeosciences. 8(2):489–503.

[18] Djavidnia S, Mélin F, (2010). *Comparison of global ocean colour data records*. os.copernicus.org. 6:61–76.

[19] Werdell PJ, Franz BA, Bailey SW, Harding, Jr. LW, Feldman GC. (2007). *Approach for the long-term spatial and temporal evaluation of ocean color satellite data products in a coastal environment*. In: Coastal Ocean Remote Sensing. p. 66800G.

[20] Taylor KE. (2001). *Summarizing multiple aspects of model performance in a single diagram*. Journal of Geophysical Research Atmospheres. 106(D7):7183–92.

[21] Belo Couto A, Brotas V, Mélin F, Groom S, Sathyendranath S. (2016). *Inter-comparison of OC-CCI chlorophyll-a estimates with precursor data sets.* International Journal of Remote Sensing. 37(18):4337–55.

[22] Moradi M. (2021). *Evaluation of merged multi-sensor ocean-color chlorophyll products in the Northern Persian Gulf.* Continental Shelf Research. 221:104415.

[23] Al Shehhi MR, Gherboudj I, Ghedira H. (2014). *An overview of historical harmful algae blooms outbreaks in the Arabian Seas*. Marine Pollution Bulletin. 86(1–2):314–24.

[24] Moradi M, Kabiri K. (2012). *Red tide detection in the Strait of Hormuz (east of the Persian Gulf) using MODIS fluorescence data*. International Journal of Remote Sensing. 33(4):1015–28.

[25] Richlen ML, Morton SL, Jamali EA, Rajan A, Anderson DM. (2010). *The catastrophic 2008-2009 red tide in the Arabian gulf region, with observations on the identification and phylogeny of the fish-killing dinoflagellate Cochlodinium polykrikoides*. Harmful Algae. 9(2):163–72.

[26] Moradi M. (2020). *Trend analysis and variations of sea surface temperature and chlorophyll-a in the Persian Gulf.* Marine Pollution Bulletin. 156.

[27] Moradi M, Moradi N. (2021). *Correlation between concentrations of chlorophyll-a and satellite derived climatic factors in the Persian Gulf*. Marine Pollution *Bulletin*. 16